Soils and Rocks
www.soilsandrocks.com
An International Journal of Geotechnical and Geoenvironmental Engineering
ISSN 1980-9743
ISSN-e 2675-5475

Influence of wastewater treatment ettringite on the swelling of a soil stabilized with cement

Fernando Franco Sguarezi[1], Cláudia Telles Benatti[1],
José Renato Moreira da Silva de Oliveira[2], Juliana Azoia Lukiantchuki[1#]

Article

Keywords
Aluminum wastewater
Ettringite
Cement soil
Swelling
Unconfined compressive strength
Microstructure

Abstract

The ettringite, a highly expansive mineral that is formed when the soil is chemically stabilized, can cause structural failures due to swelling and strength loss. This study addresses the gap in understanding the incorporation of industrial effluent treatment ettringite in the swelling of soils and soil-cement mixtures. The ettringite (WTE) was produced through the chemical treatment of aluminum wastewater supplied by an industry in Maringá, Paraná, Brazil. The experimental program was conducted using lateritic sandy soil and mixtures with 5% and 6% cement and/or WTE. The swelling and strength of the studied materials were assessed using free-swelling tests and unconfined compressive strength tests. Regarding the results, the resistance decreased by approximately 86% and 71% when 5% and 6% of WTE were added to the soil-cement, respectively. The swell values for soil-cement-ettringite increased up to 21 days without a stabilization trend, and the swelling was 50-60 times that of the natural soil. The cement releases sulfate ions; consequently, ettringite formation is promoted when both cement and ettringite are present in the mixture.

1. Introduction

Chemical soil stabilization using Portland cement (PC) is widely employed to modify the properties of natural soil through pozzolanic and hydration reactions, among other intrinsic mechanisms (Freeman & Little, 1998), thereby increasing soil strength and stiffness and reducing plasticity and swelling/shrinkage. Improving soil properties enables the use of previously unsuitable soils for geotechnical applications, such as pavement layers, foundation stabilization, embankments, and slope protection, among other purposes (Dermatas, 1995; Firoozi et al., 2017; Anburuvel, 2023).

The hydration process depends on the proper amount of water, which coats the cement particles and forms a gel. In cementitious hydration, the PC constituents react with water, leading to the setting and hardening of the cement paste. However, in soils containing soluble sulfate and water, the reaction between calcium and aluminum produces ettringite and thaumasite (Firoozi et al., 2017). The ettringite $[Ca_6Al_2(SO_4)_3(OH)_{12}\ 26H_2O]$ is an expansive sulfate mineral with high crystal water content and low density, which can present a significant increase in volume during hydration. This low crystal density volume increase within the soil matrix can lead to swelling, cracking, and loss of compressive strength (Ehwailat et al., 2022; Knopp & Moormann, 2016; Taylor, 1997). The sulfate attack in soil stabilized with PC can occur through two mechanisms: 1) the PC hydration produces calcium and alumina, which react with sulfates to form ettringite, and 2) the PC hydration supplies calcium, while alumina is present in clay mineral particles. Therefore, reaction with sulfates can trigger ettringite formation (Wang, 2002). The presence of alumina in the soil impedes the prevention of sulfate attack. Several studies have shown that stabilizing soil with high sulfate content using calcium-based additives may have economic and environmental impacts on civil structures (Mitchell, 1986; Puppala et al., 1999; Ehwailat et al., 2022; Adeleke et al., 2020; Buttress et al., 2013).

The sulfate attack in soil stabilized with PC depends on pH, water availability, sulfate content, temperature, and clay minerals. In clay mineralogy, the loss of strength due to sulfate attack increases with clay content, particularly in the presence of alumina (Mitchell & Dermatas, 1992). The incorporation of lime and PC in the soil increases the pH and the solubility of silica and alumina. Consequently, the clay minerals participate in pozzolanic reactions, releasing alumina that forms ettringite (Rollings et al., 1999).

The formation of ettringite in sulfate soils creates voids between soil particles, thereby degrading soil structure. Consequently, a loss in soil resistance and linear expansion is observed (Ehwailat et al., 2022). A recent

#Corresponding author. E-mail address: jalukiantchuki@uem.br
[1]Universidade Estadual de Maringá, Departamento de Engenharia Civil, Maringá, PR, Brasil.
[2]Universidade Federal do Rio de Janeiro, Departamento de Geotecnia, Rio de Janeiro, RJ, Brasil.

Submitted on September 1, 2025; Final Acceptance on July 29, 2026; Discussion open until May 31, 2027.

Editor: Renato P. Cunha
https://doi.org/10.28927/SR.2027.014425

This is an Open Access article distributed under the terms of the Creative Commons Attribution license (https://creativecommons.org/licenses/by/4.0/), which permits unrestricted use, distribution, and reproduction in any medium, provided the original work is properly cited.

study by Ribeiro et al. (2025) found ettringite formation in cement-treated sediments after a curing period of up to 90 days. The authors discussed the importance of long-term curing in assessing the durability of treated sediments. The ettringite-induced expansion during chemical stabilization of soil is a challenge; nevertheless, the effect of swelling on engineering structures is well known. Several studies have used an industrial waste, blast furnace slag (BFS), ground into fine particles, to suppress sulfate swelling in soil stabilized with PC or lime (Frearson, 1986; Schiessel & Haerdtl, 1994; Wild et al., 1999; Li et al., 2020). Results show that a small amount of BFS can reduce swelling damage and prevent deleterious effects on strength (Wild et al., 1996; Higgins, 1998; Li et al., 2020). Cementitious materials, such as silica fume (Ebailila et al., 2022), amorphous silica waste (Wang et al., 2001), liquid ionic stabilizer (He et al., 2018), geopolymers based on metakaolin and fly ash (Suraj et al., 2020), and nanotechnology products (Eyo et al., 2021), can be used to control the ettringite-induced expansion.

Puppala et al. (2005) investigated ettringite mineral formation by producing the mineral under laboratory conditions. Experimental tests were conducted on a lime-treated soil specimen using ionic water (alumina and sulfate) to induce ettringite formation. The free-swelling results show that soil specimens with synthesized ettringite exhibited less swelling than those without ettringite. According to the authors, the results were attributed to the mineral's needle shape, which induces interlocking attraction. The dispersive forces developed during water adsorption are less than the interlocking forces between ettringite and soil particles. The authors also noted that another explanation is that the water may not have migrated into the interlayers to achieve sufficient hydration to induce swelling. Additionally, a recent study demonstrated that nano-ettringite improved hydration kinetics, rheological and microstructural behavior, and increased the strength of cement paste in the early stages (Halder et al., 2025)

The chemical treatment of aluminum wastewater, which contains phosphates and sulfates from the anodizing industry, can also generate the mineral ettringite. Discharge of aluminum wastewater into the environment can alter the sulfur cycle and affect the characteristics of receiving waters (Benatti et al., 2009). Therefore, removing sulfate from industrial effluent via ettringite formation is a desirable solution, as it is a simple and low-cost process. However, recent studies have highlighted the importance of implementing options for reuse (Rios et al., 2024; Nikolova et al., 2025; Zhao et al., 2026).

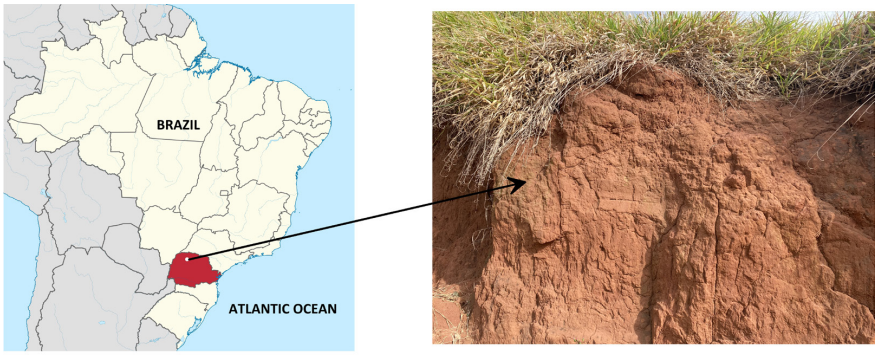
Therefore, this paper presents a novel experimental study on the swelling effects of incorporating ettringite produced by industrial wastewater treatment (WTE) into a lateritic soil stabilized with PC. The research was conducted to evaluate the geotechnical properties, including unconfined compressive strength, free swelling, and microstructure of the soil mixtures. Although several studies on ettringite formation in soil-cement mixtures have been conducted, only a few have evaluated the effect on the swelling caused by WTE incorporation on these mixtures.

2. Materials properties and methods

2.1 Materials properties

The lateritic soil is from a site near Mandaguaçu, Paraná, Brazil. The lateritic clayey sand is from the Caiuá Formation and consists of fine- to very-fine sandstone (Figure 1). The geotechnical characterization of the natural soil is presented in Table 1. The soil exhibited a low sulfate content (17.4 ppm), compared with expansive soils (Puppala et al., 2005). The method for estimating sulfate content involves extracting sulfate from phosphate ions dissolved in acetic acid and quantifying sulfur using a colorimeter or spectrophotometer.

The CP II-Z-32 Portland cement, in addition to clinker, contains calcium sulfates and pozzolans. The particle diameters range from 10 to 100 μm, and the specific gravity of the grain is 3.045.



(a) (b)

Figure 1. Lateritic soil from Mandaguaçu city (Paraná state): (a) Mandaguaçu city located in the Paraná state; (b) Lateritic red latosol profile.

The pretreated aluminum wastewater was collected from an anodizing industry in Maringá, Paraná, Brazil. The pre-treatment consists of a physicochemical coagulation process using polyaluminum chloride (PAC) and a cationic polymer as flocculants. The pH was measured to confirm the solution's alkaline behavior. The sulfate concentration was measured using a spectrophotometer (HACH), model DR2800.

The ettringite samples were synthesized at the Laboratory of Environmental Sanitation (UEM) from pre-treated aluminum wastewater (Figure 2). For the sulfate content reduction, aluminum hydroxide ($Al(OH)_3$ p.a) and calcium chloride ($CaCl_2 \cdot 2H_2O$ p.a) were added to the pre-treated aluminum wastewater. The stoichiometric ratios, based on the initial sulfate concentration, for calcium and aluminum were $[Ca^{2+}]:[SO_4^{2-}] = 2$ and $[Al^{3+}]:[SO_4^{2-}] = 0.4$, and were used to calculate the quantities of reagents in the adopted molar ratio.

The chemical reagents (Figure 2a) were added to the pretreated wastewater, and the solution was agitated in a Jar test for 30 minutes (Figure 2b). The solution was left undisturbed for 24 hours to allow the solids to precipitate (Figure 2c). Subsequently, the supernatant was removed, and pH and sulfate concentration were measured to assess the method's suitability. The sludge was dried in an oven at 115°C for 48 hours (Figure 2d), reaching an ettringite sample. The initial sulfate content in the wastewater was reduced by approximately 90%, indicating the suitability of the ettringite precipitation treatment. The micrograph of WTE (Figure 3) is consistent with spherical ettringite crystals reported in previous studies (Rindle et al., 2025; Frederickx et al., 2025).

Table 2 summarizes the chemical composition of the materials studied. The soil is predominantly composed of SiO_2 (silicon dioxide) due to the presence of quartz. Additionally, Al_2O_3 and Fe_2O_3 (iron and aluminum oxides) were detected, confirming the soil's lateritic behavior. The PC is predominantly composed of CaO (Calcium oxide) due to the lime addition in the clinker and SiO_2 from the pozzolan used in CP II Z. The chemical composition of WTE shows the predominant presence of CaO and SO_3 (Sulfur trioxide), which agrees with the molecular structure of the mineral and information from previous work. Cl and Al are associated with the chemical reagents calcium chloride and aluminum hydroxide used in the production of ettringite.

The X-ray diffraction (XRD) pattern (Figure 4) shows that the PC is composed of calcite, muscovite, gypsum, aluminum oxide, quartz, and anhydrite, among other minerals. The results are in accordance with PC CP II Z-32 (Table 2). The XRD pattern of WTE detected ettringite, anhydrite, hydrated calcium silicate, and portlandite. The presence of such minerals is justified, as ettringite forms from calcium sulfate and hydrated aluminum. The mineralogical soil composition indicated feldspar, quartz, and low activity clay minerals (kaolinite and halloysite). The lateralization process of tropical soils accounts for the presence of magnetite, iron oxides, hematite, and aluminum oxides.

Table 1. Geotechnical parameters of the natural soil.

Geotechnical parameters	Soil
Liquid limit (%)	25
Plastic limit (%)	13
Plasticity index (%)	12
Particle density (ρ_s)– fine fraction (kN/m^3)	26.3
Fine gravel (%)	-
Coarse sand (%)	-
Medium sand (%)	-
Fine sand (%)	72
Silt (%)	6
Clay (%)	22
Mean particle diameter - D_{50} (mm)	0.16
Uniformity coefficient	-
Curvature coefficient	-
Sulfate content (ppm)	17.4

where: ρ_s is the particle density; D_{50} is the mean particle diameter.

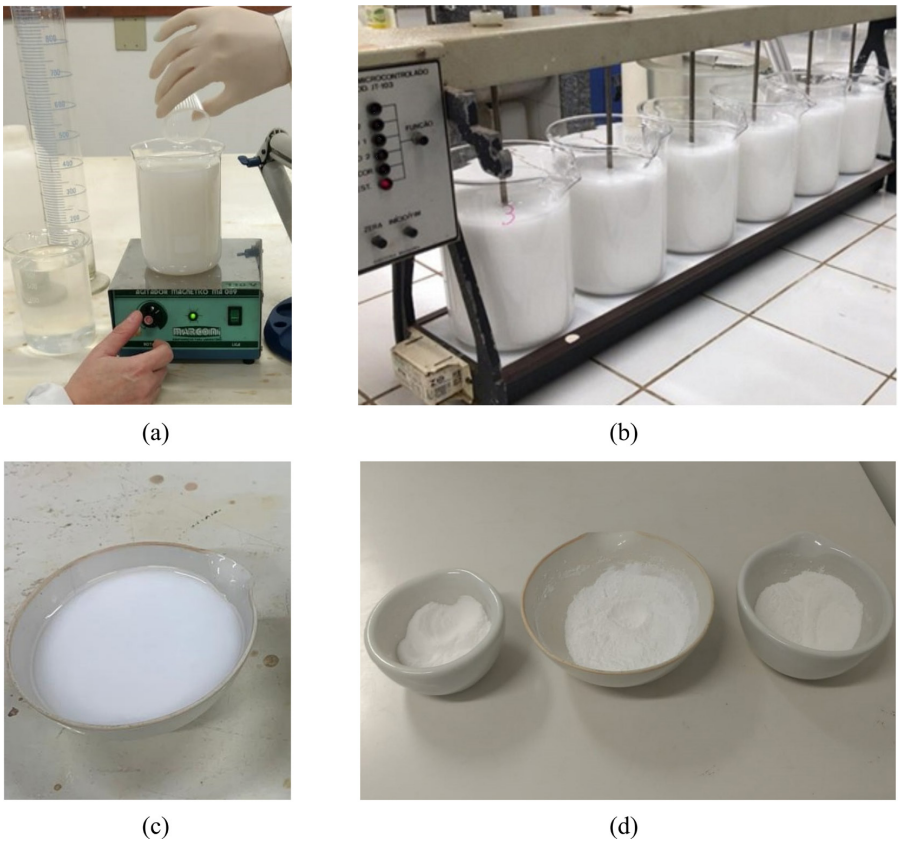
2.2 Mixtures

The proportions of PC and WTE used for mixture preparation, as reported in a previous study (Rios et al., 2024),

Table 2. X-ray fluorescence (XRF).

Component	Soil (%)	Portland cement (%)	Ettringite (%)
Al_2O_3	32.3	8.17	4.04
SiO_2	42.5	23.00	5.46
SO_3	0.512	5.12	29.10
CaO	0.308	52.70	44.10
TiO_2	3.34	N.I (1)	N.I(1)
MgO	N.I (1)	3.00	0.15
Cl	N.I (1)	0.22	11.90
K_2O	N.I (1)	1.47	1.63
Fe_2O_3	20.7	6.06	0.75
Na_2O	N.I (1)	N.I (1)	2.28
Total	99.66	99.74	99.41

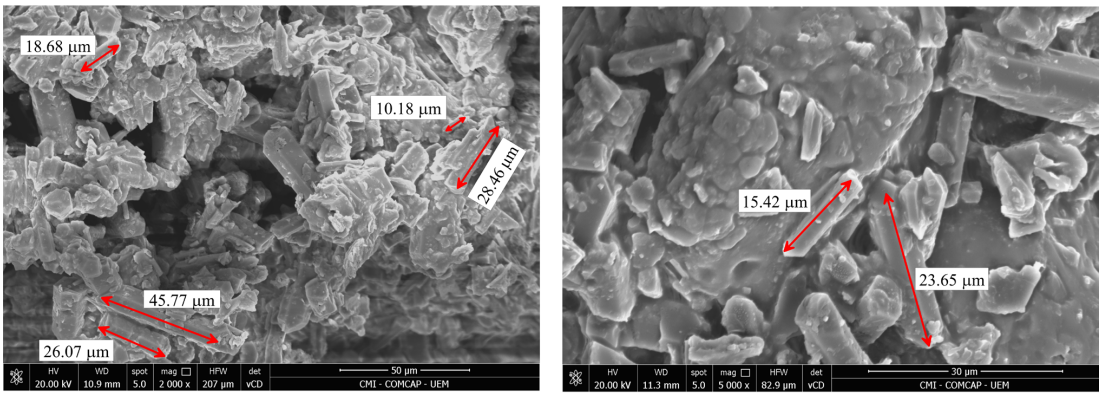
(1) N.I is when the chemical element was not identified.



(a) (b)

(c) (d)

Figure 2. Stages of ettringite production: (a) addition of chemical reagents; (b) agitation of the solution through Jar test equipment; (c) solution in rest for solids precipitation; (d) ettringite produced after 48 hours drying in an oven.



(a) (b)

Figure 3. Micrograph of synthesized ettringite (WTE) and crystal identification: (a) 2000 ×; (b) 5000 ×.

are presented in Table 3. The amounts of the materials were calculated using the dry mass as the reference. The natural soil was mixed with PC and WTE at the predefined material amounts (Figure 5). Then, the materials were mixed and sieved through a #2.0 mm sieve to form a homogeneous mixture. Subsequently, water was added in an amount corresponding to the mixture's optimum water content. The mixture was homogenized again to prepare the test samples. Tests were conducted to assess the influence of WTE incorporation on soil-cement mixtures. Unconfined compressive strength (UCS), free-swelling strain tests, and microstructural analysis were conducted to evaluate the mixture's behavior.

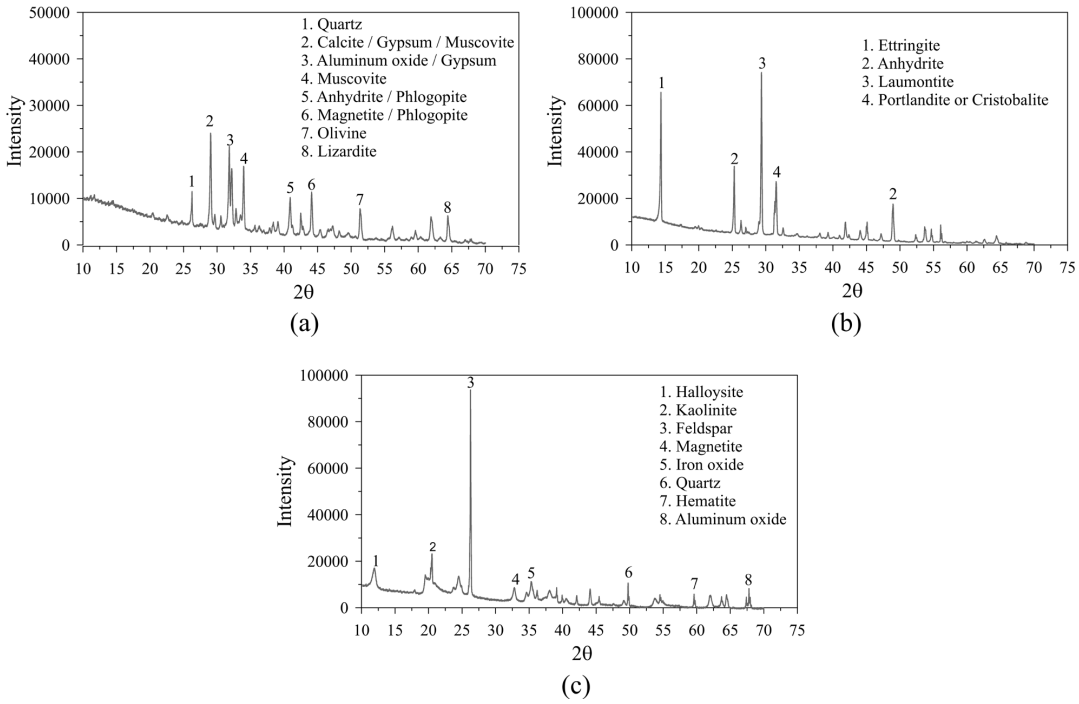


Figure 4. X-ray diffraction patterns: (a) PC (CP II Z-32); (b) WTE; (c) Natural soil.

Table 3. Mixtures characteristics used for experimental tests.

Materials	Soil (%)	WTE (%)	PC(%)
S_0	100	-	-
SE_5	95	5	-
SE_6	94	6	-
SC_5	95	-	5
SC_6	94	-	6
SC_5E_5	90	5	5
SC_6E_6	88	6	6

2.3 pH tests

The pH tests, in accordance with ASTM D4972 (ASTM, 2017), were conducted on natural soil and on the SC_6, SE_6, and SC_6E_6 mixtures using an aqueous solution of KCl and distilled water. The KCl solution was prepared at a concentration of 0.01 M (distilled water). The pH readings were taken after mechanical stirring in time intervals of 30 to 4320 minutes.

2.4 Specimen preparation

The compaction tests were conducted in accordance with ASTM 698-12 (ASTM, 2021a) and using the Brazilian standard effort (600 kJ/m^3). Tests were performed on the materials presented in Table 3 to assess the compaction parameters: the optimum water content (OWC) and the maximum dry unit weight (MDW). The specimens were molded to estimate the MDW and OWC of the soil or soil mixture, using the respective compaction curves as references. The amounts of the materials (Table 3) were calculated from their dry weights. For UCS tests, the specimens were prepared with 50 mm and 100 mm of diameter and height, respectively (Figure 6a). For the swell tests, the specimens were prepared with 50 mm and 20 mm of diameter and height, respectively (Figure 6b). The specimens with cement were wrapped and kept in a wet room for 7 days.

2.5 Unconfined compressive strength (UCS)

The UCS tests on the materials were performed in accordance with ASTM D2166-06 (ASTM, 2006), and the

CC BY



Figure 5. Materials mixed for sample preparation: (a) soil-cement mixture; (b) soil-cement-ettringite mixture.

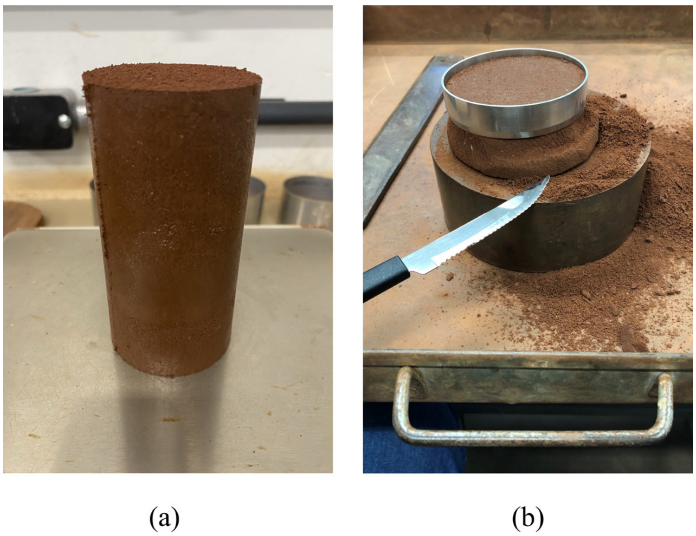


Figure 6. Specimen for experimental tests: (a) UCS tests (50 × 100 mm); (b) Swell tests (50 × 20 mm).

compressive strength (*qu*) was calculated as the average of four samples tested. Before testing, the specimens with PC were submerged for 24 hours to increase saturation and reduce suction-induced effects on the *qu* values. The average degree of saturation was estimated to be 89% based on the specimen properties. The *qu* results exhibit a coefficient of variation less than or equal to 10%. The results were similar to those found by Rios et al. (2024), who used the same materials. Therefore, the data's statistical representativeness was considered satisfactory.

2.6 Swell tests

One-dimensional free swell strain tests were conducted, based on ASTM D4546-21 (ASTM, 2021b), to evaluate the free swell behavior and estimate the swell pressure of the studied materials. The preparation of the specimens was described in section 2.4. Initially, the equipment was calibrated for the adopted load, and the test was carried out using a metallic cylinder at the specimen's location to measure the equipment's vertical displacement.

For the one-dimensional free swell strain tests, after positioning the assembled cell in the equipment, a 1 kPa load was applied. The distilled water was placed in the swell strain cell for submersion, and readings were taken at predefined time intervals in accordance with ASTM D4546-21 (ASTM, 2021b). No stabilization of readings was observed over 24 hours for the soil-cement-ettringite mixtures; therefore, a more extended test period was required, with readings taken once per day for 21 days.

The swell pressure was estimated using Method A of ASTM D 4546-21, with applied loads of 20, 50, and 100 kPa, and the specimens were submerged in distilled water after 10 min. The readings were taken until the primary swell process was complete, and the maximum strain was plotted against the corresponding load. The swell pressure is the required value to prevent the swell, corresponding to zero strain.

2.7 Scanning electron microscopy analyses (SEM)

The microstructure and cement hydration products of the stabilized specimens were evaluated using SEM analysis of small pieces of the compacted specimens cured for 7 days. The SEM tests were conducted using a Shimadzu Superscan SS-550 microscope, which provides magnifications ranging from 20 to 300,000.

3. Results and discussion

3.1 Cement and ettringite's influence on the chemical parameters

Figure 7 shows the pH, ΔpH, and point of zero charge (PZC) values of the soil and mixtures containing 6% Portland cement and/or ettringite. The pH of natural soil increases with the incorporation of PC and WTE (Figures 7a and 7b), reaching a maximum of 12.3, which is slightly lower than that of KCl. Chew et al. (2004) reported that the pH increases more rapidly at lower cement content than at higher cement content. The increase in pH is due to K^{+}, which concentrates at the clay surface and forms a flocculated soil-cement matrix. Mengue et al. (2017) also observed a significant increase in pH for lower cement contents. A pH of 12.4, achieved with 6% cement, provides adequate conditions for developing cement hydration. However, when the pH reaches approximately 9, the solubility of silica and alumina increases, and the clay particles produce active alumina, enabling the environment to form ettringite and sulfate attack (Rollings et al., 1999).

The S_0, SE_6, and SC_6E_6 mixtures exhibit negative ΔpH values, indicating the predominance of negative charges on the particle surface. The point of zero charge (PZC) was estimated using a simplified approach proposed by Uehara

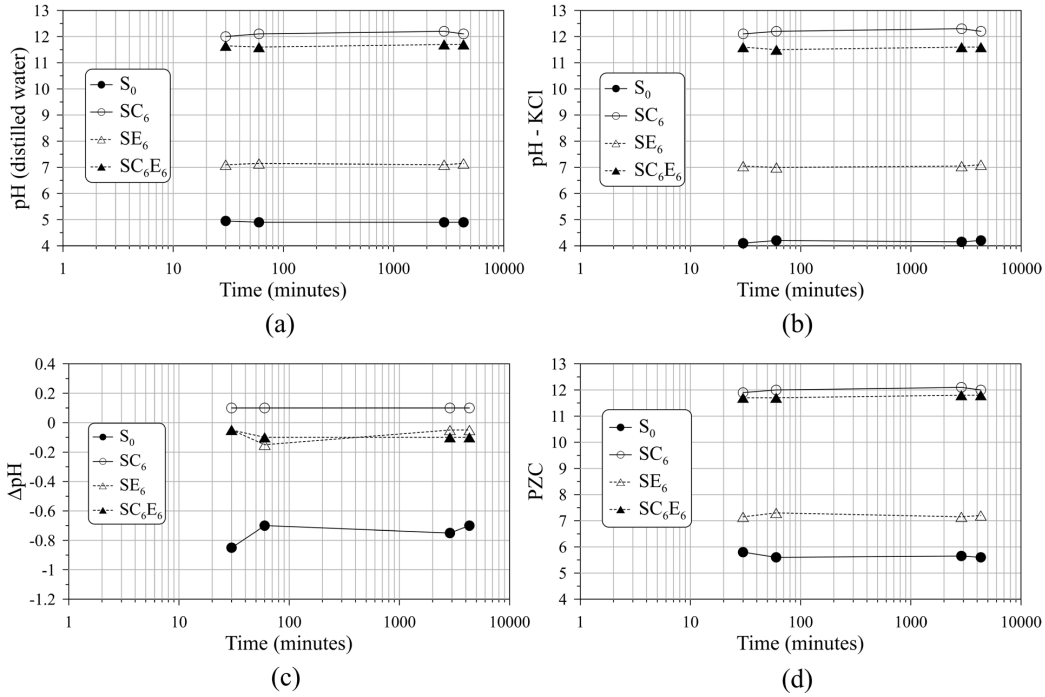


Figure 7. Variation of chemical parameters: (a) pH in distilled water; (b) pH in KCl; (c) ΔpH; (d) PZC with cement and ettringite incorporation.

CC BY

& Gillman (1981). Results show that the PZC and pH in distilled water for SE_6, SC_6E_6, and SC_6 are very similar, whereas for S_0, a pH of 5.65 was obtained, higher than the pH in distilled water. The PZC estimation indicates that the natural soil is negatively charged.

3.2 Compaction parameters

Figure 8 shows the compaction curves of the studied materials, indicating that the MDW and OWC were 19.22 kN/m^3 and 11.80%, respectively, for the lateritic soil. Results also show that the MDW of the natural soil increased when cement and/or ettringite was added, while the OWC decreased when ettringite or cement-ettringite was added. For cement incorporation, the OWC increases with cement content. Nazari et al. (2021) also reported that incorporating Portland cement increases the OWC; however, the authors observed that the MDW decreases with increasing cement content. The specific gravity of ettringite and cement is higher, and their particle sizes are significantly smaller than those of the natural soil, which justifies the increase in MDW.

3.3 Unconfined compressive strength (*qu*) versus ettringite and cement content

The typical axial stress-strain curves from UCS tests of the studied materials are shown in Figure 9a. The stress-strain curve of natural soil shows no significant reduction in resistance after failure. On the other hand, incorporating PC into natural soil altered the stress-strain curve, leading to brittle failure behavior. The results are similar to those of previous studies (Estabragh et al., 2018; Saroglou, 2009; Alkiki et al., 2021; Lade & Trads, 2015), indicating that cement incorporation changes the *qu* of the soil. However, no significant difference was noticed in *qu* values when 5-6% of cement was used. The *qu* increases by 10-11 times when cement is added to natural soil due to the pozzolanic reaction among soil, cement, and water. The products of cement hydration, namely calcium aluminate hydrate (CHA) and calcium silicate hydrate (CSH), promote intercluster bonding and fill the voids between soil particles; consequently, strength increases (Alkiki et al., 2021). The CSH flocculated gels, formed during cement hydration, coat soil particle surfaces, forming clusters (Figure 9b). The presence of calcium alumino-ferrite hydrate crystals (AFt) and monosulfate calcium sulfoaluminate hydrate crystals (AFm) can also be detected.

Figure 10a and Figure 10b show the relation between the cement content (a) or the cement-ettringite content (b) and the strength values. In both situations, the *qu* values increased with the addition of cement. However, when the ettringite is added to soil-cement mixtures, the *qu* values decreased by about 86% and 71% for 5% and 6% of ettringite, respectively. As ettringite is a calcium and aluminum-hydrous sulfate, its incorporation into soil-cement mixtures can serve as an internal source of sulfate, leading to sulfate attack and delayed

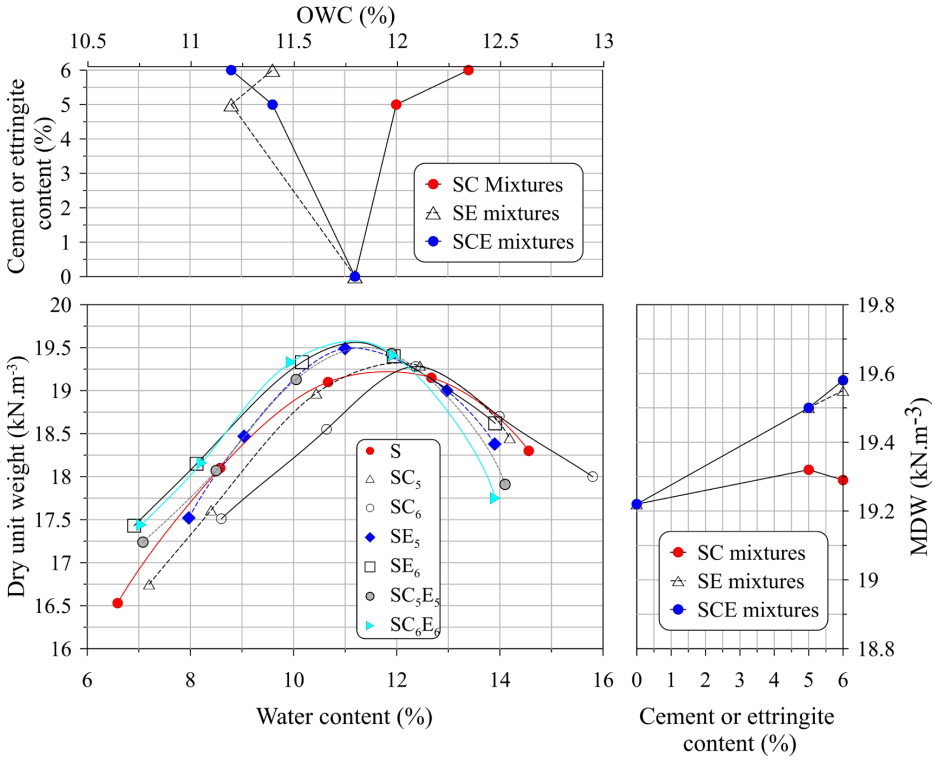


Figure 8. Compaction curves and compaction parameters (OWC and MDW) as a function of cement and/or ettringite content.

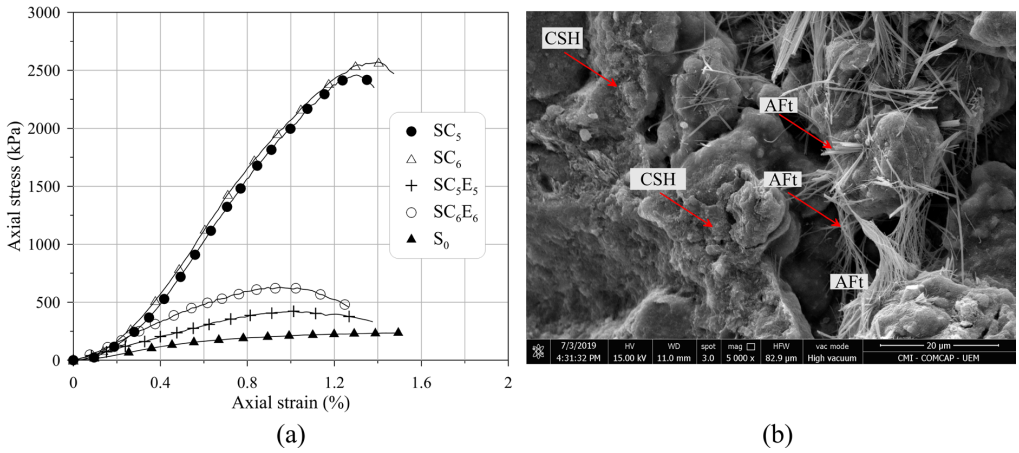


Figure 9. Unconfined compressive strength results: (a) Axial stress-strain curves for the studied materials; (b) SEM image of the SC6.

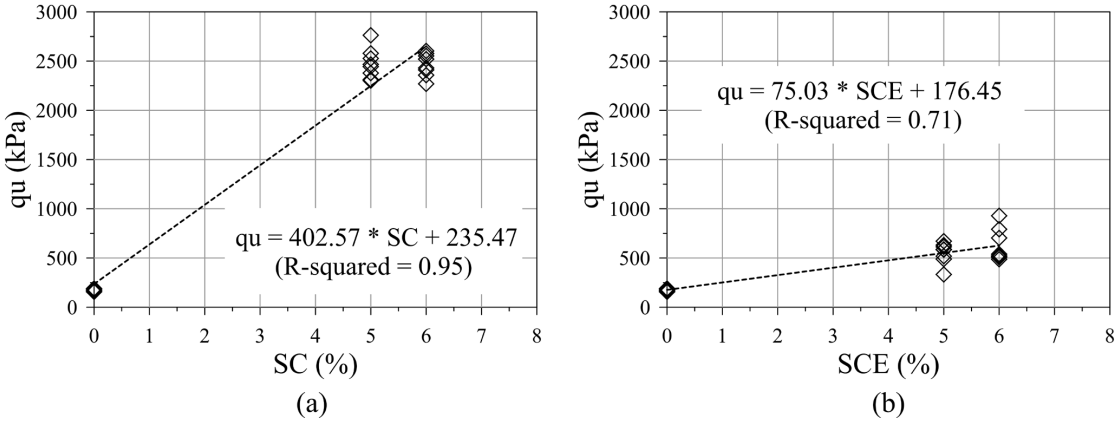


Figure 10. UCS strength results: (a) *qu* versus cement content; (b) *qu* versus cement-ettringite.

ettringite formation (DEF). Rios et al. (2024) observed that although ettringite does not affect soil resistance when used simultaneously with cement, the performance of soil cement is impaired because ettringite inhibits cement hydration and hinders the increase in soil cement strength.

3.4 Porosity and cement-ettringite effect on the unconfined compressive strength (*qu*)

The porosity effect in the studied mixtures was evaluated by considering two critical variables: porosity (η) and the voids-to-cement ratio (C_{iv}), a parameter proposed by Consoli et al. (2007). The *a* exponent expresses the rate of increase of *qu* as a function of η and C_{iv}, consequently, the relation of *qu* versus $\eta/(C_{iv})$ is optimized (Consoli et al., 2007; Consoli et al., 2009). Figure 11 shows the relationship between the UCS and $\eta/(C_{iv})^a$ for soil-cement and soil-cement-ettringite mixtures with an exponent value of 0.20. The experimental data used to adjust the *a* exponent show that the *qu* for soil-cement-ettringite can be predicted by / $(C_{iv})^{0.20}$ using the Consoli et al. (2007) approach based on a single dosage curve. The η and C_{iv} were determined based on the characteristics and dosages of the materials used during sample preparation. Equation 1, used to estimate the unconfined compressive strength, presents *qu* as a function of $\eta/(C_{iv})^{0.20}$ with a coefficient of determination (R^2) of about 0.74.

$$qu = 10.55 \times 10^6 \left[\frac{\eta}{(C_{iv})^{0.20}} \right]^{-0.148} \quad (1)$$

3.5. One-dimensional free swell and microstructure results

The free-swell values for the studied materials were calculated by subtracting the equipment offset from the measured vertical displacement. The results were divided by

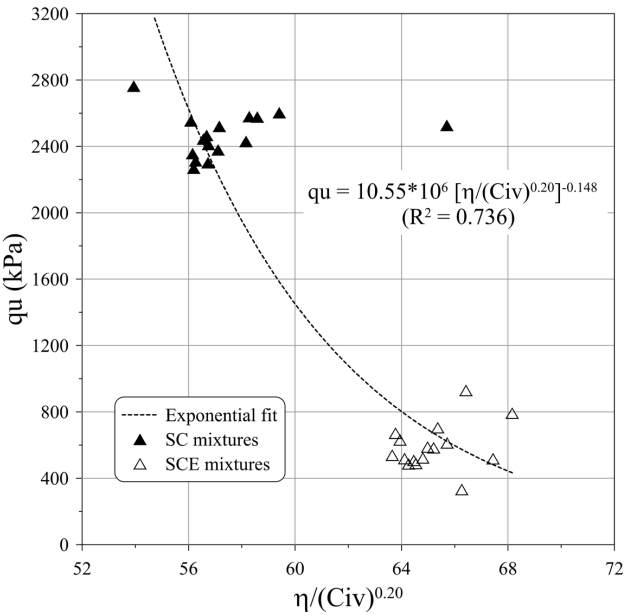


Figure 11. UCS strength versus $\eta/(Civ)^a$ index.

the metallic ring height (20.0 mm). Figure 12a presents the average (continuous line) and the individual (dashed line) test results. As expected, the S_0 shows an average swell of 0.30%, which remained constant after 8 hours (Figure 12a). The S_0 can be classified as a low-swelling potential soil (Chen, 1988; Yilmaz, 2006), as confirmed by the plasticity index (*PI*) and XRD results. The kaolinite clay mineral is frequently detected in soils with low swell potential (Prakash & Sridharan, 2004).

The incorporation of Portland cement (SC_5) in the S_0 reduced the free swell by about 83% (Figure 12b). Chemical additives, such as cement, have demonstrated an excellent potential for controlling the expansive behavior of soils (Barman & Dash, 2022). Rai et al. (2021) reported a reduction of 49.75% in the free swell index when 6% of cement and 15% of fly ash were added to a sandy silt.

The microstructure of the natural soil (Figure 13a) shows the presence of unhydrated granular particles (quartz), lamellar materials identified as clay minerals (kaolinite), and small pores (voids). The presence of these minerals agrees with the X-ray diffraction pattern of natural soil (Figure 4). However, upon PC addition, a cementitious gel formed around the granular particles and the clay minerals (Figure 13b). Cementitious hydration products, which exhibit a gelatinous appearance, significantly improve soil strength (Barman & Dash, 2022). Several studies indicate that cement incorporation reduces the soil plasticity, liquid limit, and swelling potential. In contrast, the shrinkage limit and the soil strength tend to increase (Barman & Dash, 2022; Chew et al., 2004).

The incorporation of 5% and 6% ettringite into the natural soil (Figure 12c) increased the free-swelling values, with a slight tendency toward stabilization after 24 hours. The maximum average swell values were 0.63% and 0.80% for SE_5 and SE_6, respectively, approximately 2.3 times those of the natural soil. The swelling of the soil-ettringite mixture is related to the material's interaction. The presence of the AL_2O_3 (Table 2), the kaolinite clay mineral, and the SO_4 (Table 2) promotes the ettringite-induced swelling. Mehta (1973) noted that colloidal ettringite attracts water molecules, thereby inducing interparticle repulsion and overall expansion. However, Puppala et al. (2005) observed that the swell values for compacted specimens using 8% of the synthesized ettringite were lower than those of the soil specimens without ettringite. According to the authors, the reduction in soil swelling can be attributed to interlocking forces arising from the ettringite needle shape, which reinforce soil particles. The complex water migration that induces hydration of the interlayers of compacted specimens with ettringite, and the swelling itself, can also be associated with low swell values (Puppala et al., 2005). The identification of needle-shaped crystals in the soil-ettringite mixtures (Figure 14) was based on a previous study (Krivoborodov et al., 2023), and their swelling is associated with the oriented growth of ettringite crystals (Ogawa & Roy, 1982).

Results also show that the simultaneous incorporation of 5% and 6% cement and ettringite into the natural soil (Figure 12d) alters the behavior of the free-swelling curve. Initially, the curves are similar to those of the natural soil because the cement hydrates in water, whereas ettringite does not hydrate or swell. However, after 8 hours, the curves' behavior changed markedly, and the values increased sharply over 24 hours. Additional tests for SC_5E_5 and SC_6E_6 were conducted for up to 21 days, and the materials continued to expand with no sign of stabilization (Figure 15). The final swell values were 3.25% and 2.65% for SC_5E_5 and SC_6E_6, respectively, representing about 50-60 times those of the natural soil. Knopp & Moormann (2016) performed swelling tests for up to 100 days, showing that initial swelling is due to hydration effects, followed by stagnation, after which a significant increase in swelling is associated with ettringite formation. A stabilization trend was observed for the soil-ettringite mixtures after a stagnation period (8 hours) (Figure 15), and afterward, the swelling increased. However, for the soil-ettringite-cement mixtures, the swell values increased up to 21 days. One explanation is the delayed ettringite formation (DEF), which originates from internal sulfate attack. DEF causes expansion, cracking, and loss of resistance, affecting the material's performance. The incorporation of PC into the soil-ettringite mixture releases sulfates and aluminates, which, under ideal conditions of temperature and moisture, can react to form expansive ettringite. However, confirmation of DEF presence is not a simple analysis and requires further microscopy studies, and it may be associated with a synergistic catalysis phenomenon.

Figure 16 presents the microstructure of the SC_6E_6, where a large random distribution of crystals can be observed

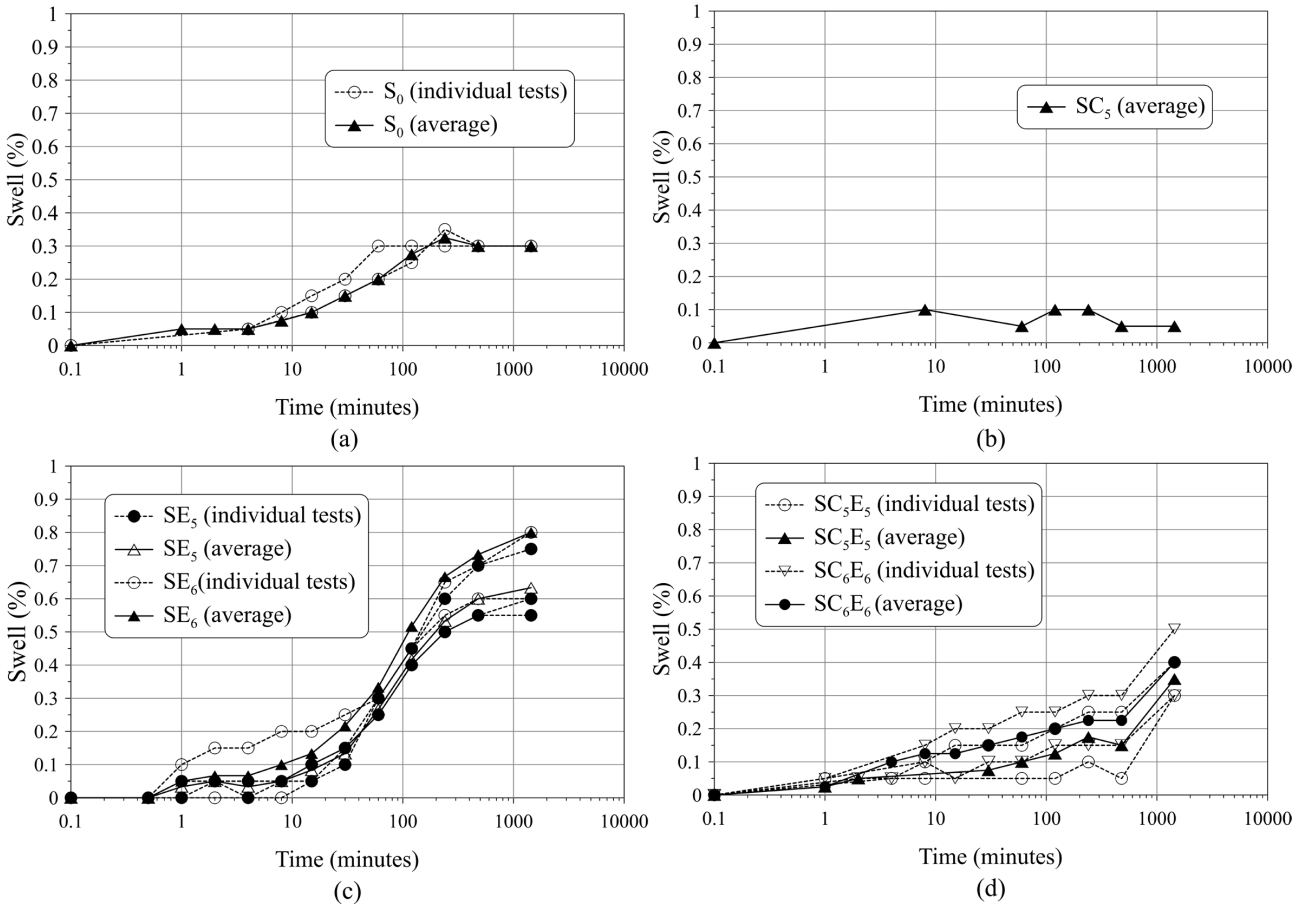


Figure 12. Swell curves for the studied materials: (a) natural soil; (b) soil-cement mixture; (c) soil-ettringite mixtures; (d) soil-cement mixture.

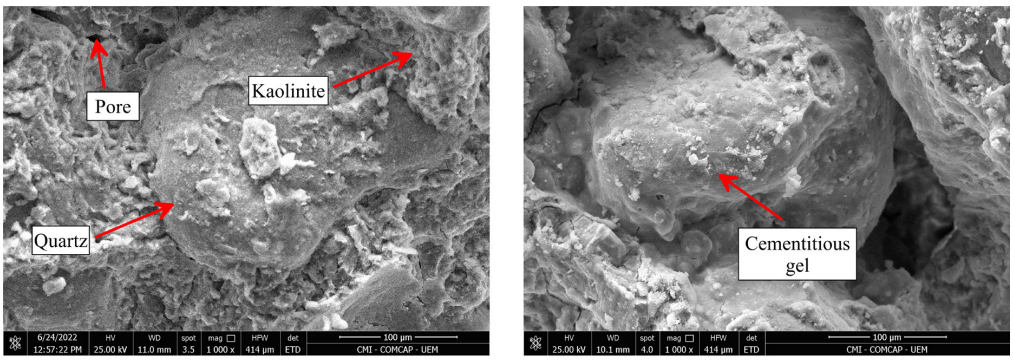


Figure 13. Microstructure: (a) natural soil (S_0) – 1000 ×; (b) soil-cement mixture (SC_6) – 1000 ×.

(Figure 16a). The filled voids and the crystal size are higher than those observed for the SE_6 mixture (Figure 14). The swell depends on the amount and the size of the crystals, which explains the higher values of the SC_5E_5 and SC_6E_6 mixtures. The results also show that the swell pressure of the SCE mixtures was higher than that of the SC mixtures. For SC_5 and SC_6, the swell pressures were 10.0 kPa and 13.0 kPa, respectively, while 18.3 kPa and 17.6 kPa for SC_5E_5

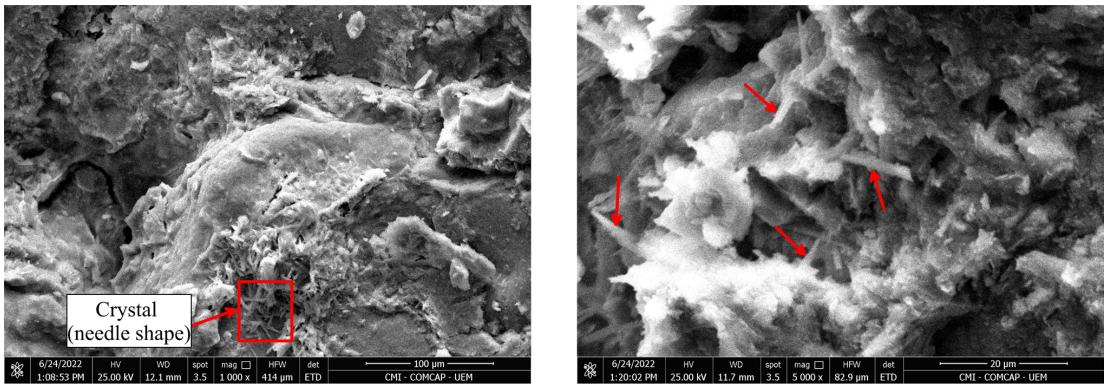


Figure 14. Microstructure of soil-ettringite mixture (SE_6): (a) 1000 ×; (b) 5000 ×.

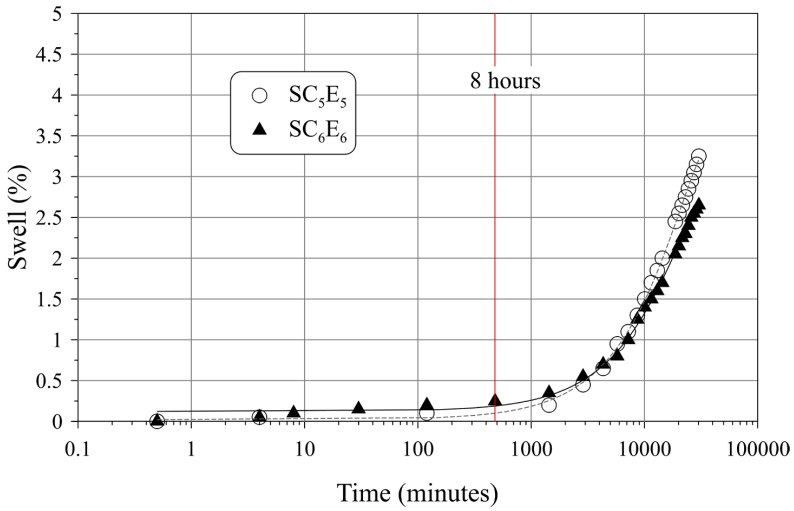


Figure 15. Swell curves for the SC_5E_5 and SC_6E_6 (21 days).

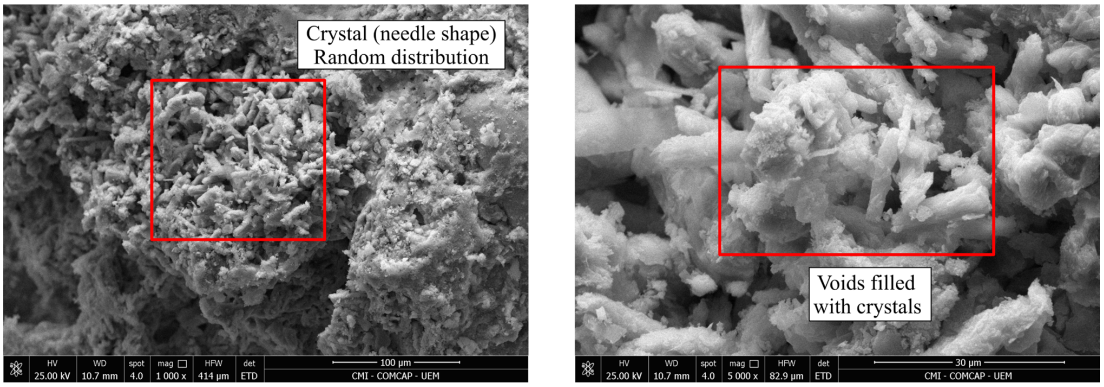


Figure 16. Microstructure of soil-ettringite mixture (SC_6E_6): (a) 1000 ×; (b) 5000 ×.

and SC_6E_6, respectively. The SCE mixtures presented a higher amount of ettringite crystals than the SE mixtures. Consequently, as expected, the swell pressure increases.

4. Conclusion

It is very important to find solutions for the wastewater generated by the aluminum anodizing industry, which contains high levels of phosphates, sulfates, nitrates, and aluminum. The discharge of wastewater into the environment can alter the natural cycle of sulfur and the characteristics of the receiving water. A solution to this problem is the sulfate removal through ettringite precipitation (WTE). This paper addresses the gap in understanding the incorporation of industrial effluent treatment ettringite in the swelling of soils and soil-cement mixtures. The experimental program focused on swelling, unconfined compressive strength, and microstructure tests of soil and mixtures. The following conclusions can be stated:

1. Regarding the characterization, the pH of soil increases with the PC and WTE incorporation, reaching a maximum value of 12.3, slightly below the pH of $Ca(OH)_2$. Results show that incorporating cement and/or ettringite increases the MDW of natural soil, while the OWC decreases. For cement incorporation, the OWC increases with increasing cement content.
2. Regarding the UCS strength, values indicate that the *qu* increased when the cement was incorporated into the soil. On the other hand, soil-cement mixtures with 5% and 6% of ettringite decreased the *qu* values by about 86% and 71%, respectively. As ettringite is a calcium and aluminum hydrous sulfate, its incorporation into soil-cement mixtures can act as an internal source of sulfate, causing sulfate attack and delaying ettringite formation (DEF).
3. The free swell curves show a stabilization trend for up to 24 hours for soil, soil-cement, and soil-ettringite mixtures, presenting swelling values lower than 1%. However, the simultaneous incorporation of 5% and 6% cement and ettringite into the natural soil alters the behavior of the free-swelling curve. Initially, the curves resemble those of the natural soil. However, after 8 hours, the behavior changes drastically. The swell values increased sharply up to 21 days without a stabilization trend, reaching about 50-60 times those of the natural soil.
4. The microstructure of the materials shows that the ettringite crystal formation is more evident when cement and ettringite play roles simultaneously in the mixture. The PC acts as a source of sulfate ions, thereby inducing ettringite crystal formation.

In general, the laboratory test results of this research indicate that incorporating WTE into soil-cement mixtures should not be encouraged, mainly due to delayed ettringite formation and sulfate attack. However, further studies using alternative cement types, considering the ettringite hydration process and long-term field performance, must be conducted.

Acknowledgements

The authors thank the scholarship granted by CAPES (Coordination for the Improvement of Higher Education Personnel), as well as the Laboratory of Soil Mechanics, and the Laboratory of Environmental Sanitation at the State University of Maringa (UEM).

Declaration of interest

The authors have no conflicts of interest to declare. All co-authors have observed and affirmed the contents of the paper and there is no financial interest to report.

Authors' contributions

Fernando Franco Sguarezi: investigation, data curation, writing - original draft preparation. Cláudia Telles Benatti: conceptualization, methodology. José Renato Moreira da Silva de Oliveira: writing - reviewing and editing. Juliana Azoia Lukiantchuki: conceptualization, methodology, supervision, writing - reviewing and editing.

Data availability

The datasets generated and analyzed in the course of the current study are available from the corresponding author upon request.

Declaration of use of generative artificial intelligence

This work was not prepared with the assistance of Generative Artificial Intelligence (GenAI).

List of symbols

pH:	Hydrogen potential
qu:	Compressive strength
AFm:	Monosulfate calcium sulfoaluminate
AFt:	Calcium alumino-ferrite hydrate
Al:	Aluminum
$[Al^{3+}]$:	Aluminum ion
Al_2O_3:	Aluminum oxide
$Al(OH)_3$:	Aluminum hydroxide
ASTM:	American Society for Testing and Materials

CC BY

BFS:	Blast Furnace Slag
$[Ca^{2+}]$:	*Calcium ions*
$[Ca_6Al_2(SO_4)_3(OH)_{12}\ 26H_2O]$:	Ettringite
$CaCl_2.2H_2O$:	Calcium chloride
CaO:	Calcium oxide
$Ca(OH)_2$:	Calcium Hydroxide
CHA:	Calcium aluminate hydrate
(Civ)[a]:	Voids/cement ratio
Cl:	Chlorine
CP II-Z-32:	Pozzolan cement
CSH:	Calcium silicate hydrate
D_{50}:	Mean particle diameter
DEF:	Delayed ettringite formation
Fe_2O_3:	Iron oxide
$[K^+]$:	Potassium ion
K_2O:	Potassium oxide
KCl:	Potassium Chloride
LA:	Lateritic sand soil
MDW:	Maximum dry unit weight
MgO:	Magnesium oxide
Na_2O:	Sodium oxide
OWC:	Optimum water content
PAC:	Polychloride of aluminum
PC:	Portland cement
PZC:	Point of zero charge
PI:	Plasticity index
S_0:	Natural soil
SE_5:	Sample with 5% of ettringite
SE_6:	Sample with 6% of ettringite
SC_5:	Sample with 5% of Portland cement
SC_6:	Sample with 6% of Portland cement
SC_5E_5:	Sample with 5% of Portland cement and 5% of ettringite
SC_6E_6:	Sample with 6% of Portland cement and 6% of ettringite
SEM:	Scanning electron microscopy
SiO_2:	Silicon dioxide
SO_4:	Sulphate
$[SO_4^{2-}]$:	Sulfate ion
SO_3:	Sulfur trioxide
TiO_2:	Titanium dioxide
UCS:	Unconfined compressive strength (humid room for cure)
UEM:	State university of Maringá
XRD:	X-ray diffraction
XRF:	X-ray fluorescence
WTE:	Wastewater treatment ettringite
ΔpH:	Delta pH ($pH_{H2O} - pH_{KCl}$)
η:	Porosity
ρ_s:	Particle density

References

Adeleke, B., Kinuthia, J., & Oti, J. (2020). Strength and swell performance of high-sulphate kaolinite clay soil. *Sustainability (Basel)*, 12(10164), 10164. https://doi.org/10.3390/su122310164.

Alkiki, I.M., Abdulnafaa, M.D., & Aldaood, A. (2021). Geotechnical and other characteristics of cement-treated low plasticity clay. *Soils and Rocks*, 44(1), 1-13. https://doi.org/10.28927/SR.2021.053120.

Anburuvel, A. (2023). The engineering behind soil stabilization with additives: a state-of-theart review. *Geotechnical and Geological Engineering*, 42(1), 1-42. https://doi.org/10.1007/s10706-023-02554-x.

ASTM D2166-06. (2006). *Standard Test Method for Unconfined Compressive Strength of Cohesive Soil*. ASTM International, West Conshohocken, PA. https://doi.org/10.1520/D2166_D2166M-24.

ASTM D4972-01. (2017). *Standard Test Methods for pH of Soils*. ASTM International, West Conshohocken, PA. https://doi.org/10.1520/D4972-19.

ASTM D698-12. (2021a). *Standard Test Methods for Laboratory Compaction Characteristics of Soil Using Standard Effort (12,400 ft-lbf/ft3 (600 kN-m/m3))*. ASTM International, West Conshohocken, PA. https://doi.org/10.1520/D0698-12R21.

ASTM D4546-21. (2021b). *Standard Test Methods for One-Dimensional Swell or Collapse of Soils*. ASTM International, West Conshohocken, PA. https://doi.org/10.1520/D4546-14.

Barman, D., & Dash, S.K. (2022). Stabilization of expansive soils using chemical additives: A review. *Journal of Rock Mechanics and Geotechnical Engineering*, 14(4), 1319-1342. https://doi.org/10.1016/j.jrmge.2022.02.011.

Benatti, C.T., Tavares, C.R.G., & Lenzi, E. (2009). Sulfate removal from waste chemicals by precipitation. *Journal of Environmental Management*, 90(1), 504-511. PMid:18222593. https://doi.org/10.1016/j.jenvman.2007.12.006.

Buttress, A.J., Grenfell, J.R.A., & Airey, G.D. (2013). The role of ettringite in the deterioration of artificial lime stabilised soils: a microstructural study. *Road Materials and Pavement Design*, 14(3), 586-614. https://doi.org/10.1080/14680629.2013.779306.

Chen, F.H. (1988). *Foundations on expansive soils* (2nd ed.). Elsevier Science Publications.

Chew, S.H., Kamruzzaman, A.H.M., & Lee, F.H. (2004). Physicochemical and engineering behavior of cement treated

clays. *Journal of Geotechnical and Geoenvironmental Engineering*, 130(7), 696-706. https://doi.org/10.1061/(ASCE)1090-0241(2004)130:7(696).

Consoli, N., Foppa, D., Festugato, L., & Heineck, K.S. (2007). Key parameters for strength control of artificially cemented soils. *Journal of Geotechnical and Geoenvironmental Engineering*, 133(2), 197-205. https://doi.org/10.1061/(ASCE)1090-0241(2007)133:2(197).

Consoli, N., Lopes Junior, L.S., & Heineck, K.S. (2009). Key parameters for the strength control of lime stabilized soils. *Journal of Materials in Civil Engineering*, 21(5), 210-216. https://doi.org/10.1061/(ASCE)0899-1561(2009)21:5(210).

Dermatas, D. (1995). Ettringite-induced swelling in soils: state-of-the-art. *Applied Mechanics Reviews*, 48(10), 659-673. https://doi.org/10.1115/1.3005046.

Ebailila, M., Kinuthia, J., Oti, J., & Al-Waked, Q. (2022). Sulfate soil stabilisation with binary blends of lime–silica fume and lime–ground granulated blast furnace slag. *Transportation Geotechnics*, 37, 100888. https://doi.org/10.1016/j.trgeo.2022.100888.

Ehwailat, K.I.A., Ismail, M.A.M., & Ezreig, A.M.A. (2022). Ettringite formation and stabilization methods of sulfate-bearing soil: a state-of-the-art review. *Indian Geotechnical Journal*, 52(4), 927-941. https://doi.org/10.1007/s40098-022-00619-x.

Estabragh, A.R., Kholoosi, M., Ghaziani, F., & Javadi, A.A. (2018). Mechanical and leaching behavior of a stabilized and solidified anthracene-contaminated soil. *Journal of Environmental Engineering*, 144(2), 04017098. https://doi.org/10.1061/(ASCE)EE.1943-7870.0001311.

Eyo, U.E., Samuel, J.A., Samson, N., Eshmaiel, G., & Ganjian, C.E. (2021). Incorporation of a nanotechnology-based product in cementitious binders for sustainable mitigation of sulphate-induced heaving of stabilised soils. *Engineering Science and Technology, an International Journal*, 24(2), 436-448. https://doi.org/10.1016/j.jestch.2020.09.002.

Frearson, J.P.H. (1986). Sulfate resistance of combinations of Portland cement and ground granulated blast furnace slag. In *Proceedings of the 2nd International Congress on Fly Ash, Silica Fume, Slag and Natural Pozzolans in Concrete* (Vol. 2, pp. 1495-1524). American Concrete Institute Special Publication.

Frederickx, L., Phung, Q.T., & Jabbour, J. (2025). Investigation into the microstructural and mineralogical changes induced by internal swelling reactions in concrete used for nuclear power plants – a mock-up study. *Low-carbon Materials and Green Construction*, 3(1), 18. https://doi.org/10.1007/s44242-025-00083-9.

Freeman, T.J., & Little, D.N. (1998). *Develop maintenance strategy selection procedures for pavements incorporating semi-rigid or chemically stabilized layers* (No. FHWA/TX-99/1922-2). Texas Department of Transportation, USA.

Firoozi, A.A., Guney Olgun, C., Firoozi, A.A., & Baghini, M.S. (2017). Fundamentals of soil stabilization. *International Journal of Geo-engineering*, 8(1), 26. https://doi.org/10.1186/s40703-017-0064-9.

Halder, R.R., Ewuzie, U., Ogbuehi, G.I., Yusuf, A.O., Egbosiuba, T.C., & Okoronkwo, M.U. (2025). Investigating the seeding effects of nano-ettringite on the hydration and 3D microstructure of calcium sulfoaluminate cement paste. *Journal of Building Engineering*, 113, 114079. https://doi.org/10.1016/j.jobe.2025.114079.

He, S., Yu, X., Banerjee, A., & Puppala, A.J. (2018). Expansive Soil Treatment with Liquid Ionic Soil Stabilizer. *Transportation Research Record: Journal of the Transportation Research Board*, 2672(52), 185-194. https://doi.org/10.1177/0361198118792996.

Higgins, D. (1998). Soil stabilization using lime-activated ground granulated blast furnace slag. In *Proceedings of the 6th CANMENT/ACT International Conference* (Vol. 1, pp. 134-141). Bangkok, Thailand.

Knopp, J., & Moormann, C. (2016). Ettringite swelling in the treatment of sulfate-containing soils used as subgrade for road construction. *Procedia Engineering*, 143, 128-137. https://doi.org/10.1016/j.proeng.2016.06.017.

Krivoborodov, Y.R., Samchenko, S.V., Korshunov, A.V., Kozlova, I.V., & Alpacky, D.G. (2023). Increasing the hydration activity of tricalcium silicate by adding microdispersed ettringite as a nucleating agent. *Materials (Basel)*, 16(22), 7078. PMid:38005008. https://doi.org/10.3390/ma16227078.

Lade, P.V., & Trads, N. (2015). The role of cementation in the behaviour of cemented soils. *Geotechnical Research*, 1(4), 111-132. https://doi.org/10.1680/gr.14.00011.

Li, W., Yi, Y., & Puppala, A. (2020). Suppressing ettringite-induced swelling of gypseous soil by using magnesia-activated ground granulated blast-furnace slag. *Journal of Geotechnical and Geoenvironmental Engineering*, 146(7), 06020008. https://doi.org/10.1061/(ASCE)GT.1943-5606.0002292.

Mehta, P.K. (1973). Mechanism of expansion associated with ettringite formation. *Cement and Concrete Research*, 3(1), 1-8. https://doi.org/10.1016/0008-8846(73)90056-2.

Mengue, E., Mroueh, H., Lancelot, L., & Eko, R.M. (2017). Physicochemical and consolidation properties of compacted lateritic soil treated with cement. *Soil and Foundation*, 57(1), 60-79. https://doi.org/10.1016/j.sandf.2017.01.005.

Mitchell, J.K. (1986). The twentieth terzaghi lecture. *Journal of Geotechnical and Geoenvironmental Engineering*, 112(3), 255-289. https://doi.org/10.1061/(ASCE)0733-9410(1986)112:3(255).

Mitchell, J.K., & Dermatas, D. (1992). Clay soil heave caused by lime-sulfate reactions. In D. C. Hoffiman and D. D. Stanley (Eds.), *Innovations and uses for lime. STP 1135* (pp. 41-64). ASTM West Conshohocken. https://doi.org/10.1520/STP15529S.

Nazari, Z., Tabarsa, A., & Latifi, N. (2021). Effect of compaction delay on the strength and consolidation properties of cement-stabilized subgrade soil. *Transportation Geotechnics*, 27, 100495. https://doi.org/10.1016/j.trgeo.2020.100495.

CC BY

Nikolova, K.T., Bratkova, S., Angelov, A., Genova, P., Ivanov, R., & Velichkova, P. (2025). Effective laboratory-scaled ettringite precipitation of extractive waste influenced water with high sulphate content. *Ecological Engineering & Environmental Technology*, 8(8), 375-384. https://doi.org/10.12912/27197050/208581.

Ogawa, K., & Roy, D.M. (1982). C_4A_3S hydration, ettringite formation, and its expansion mechanism: II. Microstructural observation of expansion. *Cement and Concrete Research*, 12(1), 101-109. https://doi.org/10.1016/0008-8846(82)90104-1.

Prakash, K., & Sridharan, A. (2004). Free swell ratio and clay mineralogy of fine-grained soils. *Geotechnical Testing Journal*, 27(2), 220-225. https://doi.org/10.1520/GTJ10860.

Puppala, A.J., Hanchanloet, S., Jadeja, M., & Burkart, B. (1999). Evaluation of sulfate-induced heave by mineralogical and swell tests. In *Proceedings of the 9th Pan-American Conference on Soil Mechanics and Geotechnical Engineering*. Santiago, Chile.

Puppala, A.J., Intharasombat, N., & Vempati, R.K. (2005). Experimental studies on ettringite-induced heaving in soils. *Journal of Geotechnical and Geoenvironmental Engineering*, 131(3), 325-337. https://doi.org/10.1061/(ASCE)1090-0241(2005)131:3(325).

Rai, P., Qiu, W., Pei, H., Chen, J., Ai, X., Liu, Y., & Ahmad, M. (2021). Effect of fly ash and cement on the engineering characteristic of stabilized subgrade soil: an experimental study. *Geofluids*, 2021(1), 1368194. https://doi.org/10.1155/2021/1368194.

Ribeiro, I.S., Fagundes, D.F., & Nierwinski, H.P. (2025). Effects of ettringite formation on the stability of cement-treated sediments. *Resources*, 14(5), 73. https://doi.org/10.3390/resources14050073.

Rindle, O., Sixt, F., Spillane, L., Willinger, E., & Gädt, T. (2025). Revealing the morphology of nano-ettringite in cement paste: a TEM study on the influence of polycarboxylate ether superplasticizers. *Cement and Concrete Research*, 193, 107853. https://doi.org/10.1016/j.cemconres.2025.107853.

Rios, A.V.N.G., Sguarezi, F.F., Benatti, C.T., & Lukiantchuki, J.A. (2024). Influence of industrial effluent treatment ettringite on the compressive and tensile strength and microstructure of soil-cement mixtures. *Soils and Rocks*, 47(1), e2024001023. https://doi.org/10.28927/SR.2024.001023.

Rollings, R.S., Burkes, J.P., & Rollings, M.P. (1999). Sulfate attack on cement-stabilized Sand. *Journal of Geotechnical and Geoenvironmental Engineering*, 125(5), 364-372. https://doi.org/10.1061/(ASCE)1090-0241(1999)125:5(364).

Saroglou, H.I. (2009). Compressive strength of soil improved with cement. In *Proceedings of the International Foundation Congress and Equipment Expo 2009* (pp. 289-296). Orlando, FL, USA. https://doi.org/10.1061/41023(337)37.

Schiessel, P., & Haerdtl, R. (1994). Relationship between durability and pore structure properties of concrete containing fly ash. In *Proceedings of the Symposium on Durability of Concrete* (pp. 99-11). Nice.

Suraj, D.K., Priyantha, W.J., Sanjaya, S., & Branimir, S. (2020). Stabilization of highly expansive soils containing sulfate using metakaolin and fly ash based geopolymer modified with lime and gypsum. *Transportation Geotechnics*, 23, 100327. https://doi.org/10.1016/j.trgeo.2020.100327.

Taylor, H.F.W. (1997). *Cement chemist*ry. Thomas Teldford.

Uehara, G., & Gillman, G.P. (1981). *The mineralogy, chemistry and physics of tropical soils with variable charge clays*. (Westview tropical agriculture series). Boulder, Colorado: Westview Press.

Wang, L., Seals, R.K., & Roy, A. (2001). Investigation of utilization of amorphous silica residues as supplementary cementing materials. *Advances in Cement Research*, 13(2), 85-89. https://doi.org/10.1680/adcr.2001.13.2.85.

Wang, L. (2002). *Cementitious stabilization of soils in the presence of sulfate* [Doctoral dissertation]. Louisiana State University, USA.

Wild, S., Kinuthia, J.M., Robinson, R.B., & Humphreys, I. (1996). Effects of ground granulated blastfurnace slag on the strength and swelling properties of lime stabilized kaolinite in the presence of sulfates. *Clay Minerals*, 31(3), 423-433. https://doi.org/10.1180/claymin.1996.031.3.12.

Wild, S., Kinuthia, J.M., Jones, G.I., & Higgins, D.D. (1999). Suppression of swelling associated with ettringite formation in lime stabilized sulphate bearing clay soils by partial substitution of lime with ground granulated blastfurnace slag. *Engineering Geology*, 51(4), 257-277. https://doi.org/10.1016/S0013-7952(98)00069-6.

Yilmaz, I. (2006). Indirect estimation of the swelling percent and a new classification of soils depending on liquid limit and cation exchange capacity. *Engineering Geology*, 85(3-4), 295-301. https://doi.org/10.1016/j.enggeo.2006.02.005.

Zhao, B., Christodoulatos, C., Shi, Q., Ji, M., Sheets, S., & Meng, X. (2026). Effective removal of sulfate and heavy metals from wastewater by ettringite precipitation using aluminum-based sludge. *Separation and Purification Technology*, 382(Pt 2), 135776. https://doi.org/10.1016/j.seppur.2025.135776.